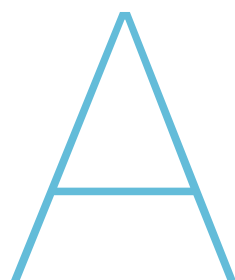


Induction of Apoptosis by Targeted Ultrasound Contrast Agents in Cancer Therapy

by Lauren J. Jablonowski, Averie M. Palovcak, and Margaret A. Wheatley, PhD

This article presents a proof-of-concept study to determine the ability to target cancer cells through the attachment of a specific ligand to ultrasound contrast agents. It represents the work of a Student Poster Presentation.



According to the American Cancer Society, more than 1.6 million new cancer cases are predicted to have been diagnosed in 2013, with approximately 35% of cases resulting in death.¹ There are numerous challenges associated with treating malignant tumors. Tumors are characterized by high interstitial pressures arising from multiple sources, including aberrant and leaky tumor vasculature, high cell density, unusual composition and structure of the tumor tissue, the composition of the extracellular matrix, and an absence of supporting lymphatic drainage structures.²⁻³ In an effort to overcome these challenges, we have previously developed drug-loaded Ultrasound Contrast Agents (UCA) consisting of microbubbles designed to shatter into nanoparticles, or nanoshards (n-Sh), and direct drug-loaded fragments into the tumor interior when insonated with ultrasound (US).⁴⁻⁸ An advantage of using micron-sized UCA as our platform is that the radiation forces exerted on the UCA by the US beam are expected to propel the UCA toward the leaky pores in the tumor vasculature, and together with the forces associated with UCA collapse caused by inertial cavitation, expel the n-Sh into the tumor for effective therapeutic delivery. This work investigates a new strategy by functionalizing these agents with a targeting ligand that is lethal upon binding to the cancer cell surface receptor. This could be achieved through ligation of

Tumor necrosis factor-Related Apoptosis-Inducing Ligand (TRAIL) to the UCA surface. The central hypothesis is that US-facilitated *in situ* inertial cavitation of TRAIL-ligated UCA generates functionalized n-Sh displaying tumor-targeting TRAIL. Upon leaving the vasculature and binding to the cancer cell surface receptors, TRAIL will initiate apoptosis in the cell via transmembrane signaling for targeted treatment.

Studies have shown that rapid angiogenesis in established tumors leads to the development of leaky capillaries, with pores measuring from 100 to 780 nm in diameter.² Coupled with the lack of lymphatic drainage, tumor-specific vasoactive factors such as vasodilators, nitric oxide and vascular endothelial growth factor promote accumulation of circulating nanoparticles in the tumor interstitium, a process termed the Enhanced Permeability and Retention (EPR) effect.⁹ Researchers are investigating methods of exploiting EPR for drug therapy.^{2,10,11} However, overall reliance on EPR is limited by slow accumulation (up to six hours), inconsistent degrees of vascular permeability between tumor types, and it is precluded entirely in some tumors that do not exhibit an EPR effect.¹¹⁻¹³ As such, numerous studies have focused on developing alternate targeting methods for drug delivery to solid tumors,^{3,14,15} and here we explore both ligand-targeting and targeting via focused ultrasound.

Passive targeting of tumors can be augmented by active targeting, which employs receptor-specific ligands. This in turn presents several challenges, including barriers preventing escape of the drug-loaded platform from the vasculature,

sufficient presentation and binding of high affinity ligands to cell-surface receptors, and problems encountered with internalization of the targeted drug.¹³ Furthermore, the choice of bioactive species employed to destroy the cancer cells is another critical factor, often involving highly toxic species that can be rendered ineffective by development of Multi-Drug Resistance (MDR). However, specific factors or ligands that trigger apoptosis uniquely in cancer cells circumvent these issues, acting as both a targeting and therapeutic entity. One such ligand is TRAIL, which selectively induces cell death in several groups of cancer cells, but not in healthy cells. Specifically, TRAIL-sensitive cancer cells express death receptors (DR4/TRAIL-R1 and DR5/TRAIL-R2) on their surface, which transmit the transmembrane apoptosis signal to the nucleus for cell death. Healthy cells, however, express decoy receptors (DcR1 and DcR2), which do not transmit this signal, effectively shielding healthy cells from this cancer therapy.¹⁶⁻²² In clinical trials, TRAIL has performed below expectations, with two possible mechanisms suggested to be the cause.^{16,23} First, bioavailability may be diminished due to non-productive binding to the decoy receptors on normal healthy cells. Second, in some cancer cell lines, there are problems with TRAIL resistance, either inherent or acquired, limiting efficacy.²⁴ Several studies also have investigated methods of overcoming this resistance, identifying compounds such as proteasome inhibitors and other drugs that can potentiate the apoptotic activity of TRAIL.²⁵⁻³⁰ In an effort to address the non-specific binding

activity of TRAIL, this study investigates the use of tumor site-specific ultrasound-targeting as the primary targeting technique, to be augmented by TRAIL binding to cancer cell surface receptors as in the usually accepted ligand targeting. Death occurs subsequent to, and as a direct consequence of, binding.

Our lab has developed hollow polymeric microspheres, made of polylactic acid (PLA) via a double emulsion process, that are highly echogenic when exposed to US.^{7,31-35} These PLA UCA are spherical, approximately 1 to 2 μm in diameter, and reach approximately 20 dB echogenicity when evaluated in vitro at low concentrations (i.e., 0.03 μg/mL).^{7,32,33} It also has been shown that US in the medical imaging range shatters drug-loaded UCA, enabling them to pass through a 400 nm pore size membrane.^{4,35} These n-Sh were measured to have an average size of 350 nm using dynamic light scattering.^{4,35,36} As such, these findings suggest that the resulting fragments can be forced through the leaky pores found in angiogenic tumor vessels (< 400 nm pore diameter), especially if the pores are also enlarged by the incident US beam.³⁷⁻³⁹ The proposed US-triggered UCA-based delivery mechanism utilizing ligated TRAIL is shown in Figure 1.

The proposed mechanism is that, when exposed to US, the UCA cavitate and burst into n-Sh. This is strongly supported by our experimental evidence.^{4,35,36} As shown in Figure 1, UCA pass freely within the vasculature until encountering the ultrasound beam, at which point they (1) experience acoustic radiation forces that push the UCA toward

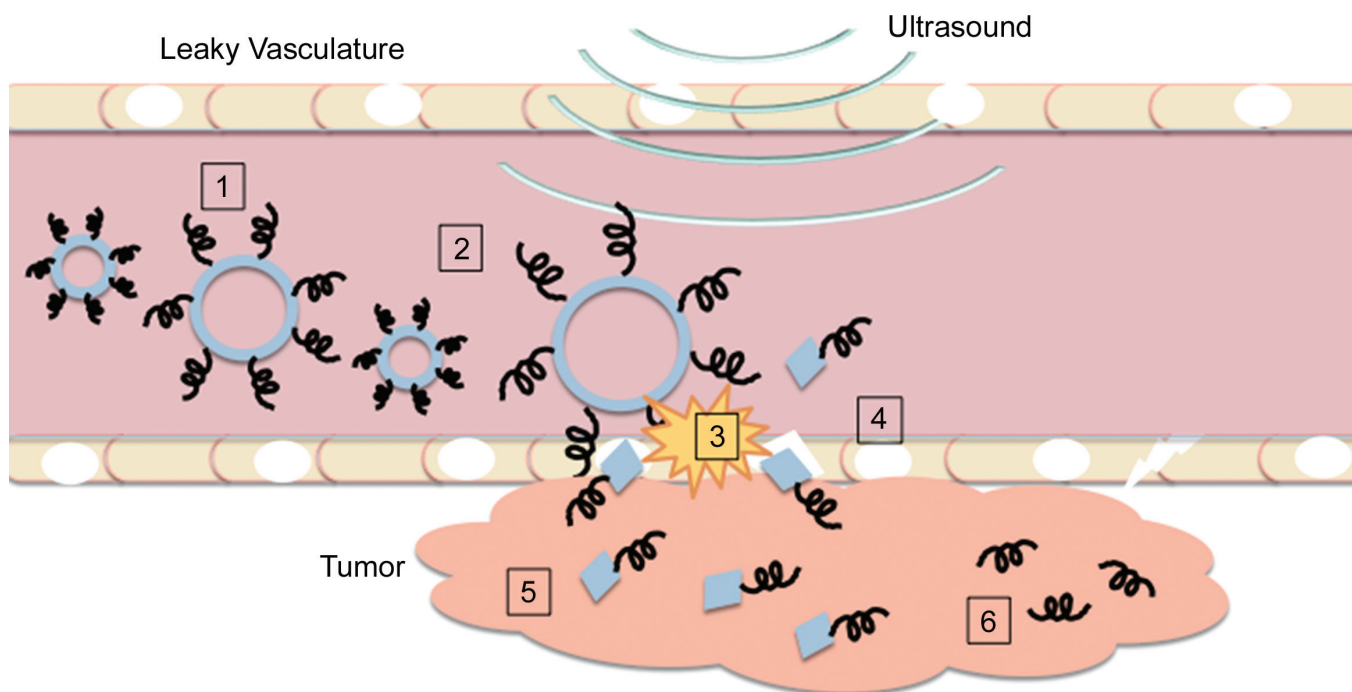


Figure 1. Schematic of ultrasound-triggered delivery using polymeric contrast agents. Blue circles represent UCA, yellow starburst indicates US-triggered UCA collapse, and black lines represent functionalizing ligands (not to scale). Refer to text for identification of numbers (1-6).

the vessel wall. The oscillating pressure wave of the US beam leads to cavitation (2) as the UCA gas core expands and contracts in response to changes in pressure. When exposed to sufficiently strong US pulses, the UCA experiences inertial cavitation, resulting in the destruction of the polymer shell (i.e., shattered UCA) (3) and *in situ* generation of n-Sh. The energy released in the process of UCA destruction is sufficient to (4) enhance the permeability of the vessel wall. The n-Sh then accumulate within the tumor interstitium (5) due to production of microjets and shear forces created when the microbubbles collapse due to inertial cavitation propelling the fragments through the vessel wall and into solid tumor tissue. There, (6) the ligated TRAIL can bind to cell surface receptors and signal for apoptosis, while the n-Sh degrade. UCA could be further modified to co-encapsulate bioactive molecules within the polymer shell, which would undergo sustained localized release as the n-Sh degrade, providing a mechanism for delivery of agents to overcome resistance.

This work describes the development of UCA coated with the targeting ligand TRAIL. These agents have the potential to generate TRAIL-ligated n-Sh at a tumor site, targeting the death cell receptors to initiate apoptosis. If successful, these UCA represent an agent capable of overcoming many of the obstacles in current chemotherapeutic methods, including reduced bioavailability, systemic toxicity, and MDR, therefore better serving the population with solid malignant tumors.

Methods

Ultrasound Contrast Agent (UCA) Preparation

UCA were prepared using the water/oil/water (w/o/w) emulsion process that has been well-established previously.⁷ Briefly, 10 mL of methylene chloride, 0.05 g camphor, and 0.5 g PLA (100 DL 7E, Evonik, (Birmingham, AL) were added to a 50 mL beaker, and stirred for 15 minutes to ensure that all of the polymer has dissolved. Then, 1 mL of 0.4 M ammonium carbamate solution was added to the organic phase and sonicated (Misonix XL2020) on ice for 30 seconds, with 1 second pauses between 3 second pulses. The first emulsion was then added to 50 mL of 5% poly(vinyl alcohol) (PVA) (25kDa, 88% mol hydrolyzed) solution kept at 4°C, and homogenized (Brinkman PT 3100 Polytron) at 9500 rpm for 5 minutes to create the second emulsion. After homogenizing, 100 mL of 2% isopropanol was added, and the solution stirred at 375 rpm for 90 minutes at room temperature to evaporate off the organic material. The remaining UCA solution was centrifuged at 5000 rpm for 5 minutes, and the pellet was collected

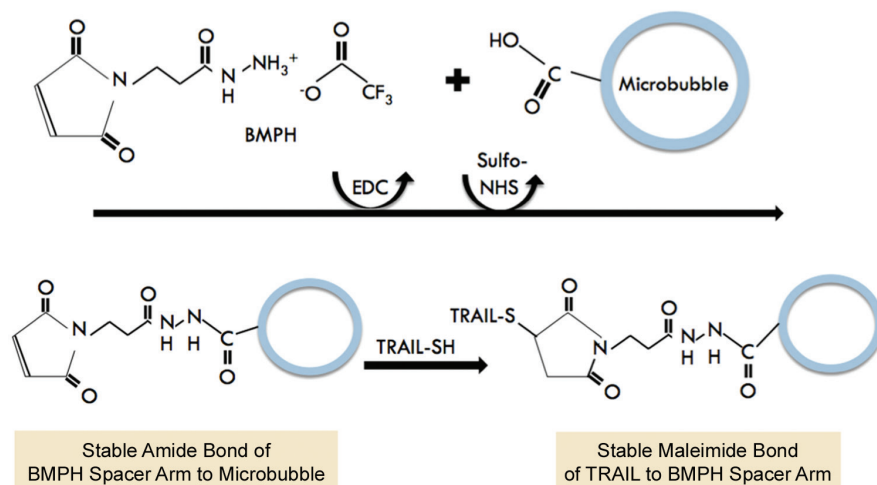


Figure 2. Maleimide reaction to bind TRAIL to the UCA surface.

and washed three times with hexane to remove any remaining organic material. After drying for 20 minutes, the UCA were washed with distilled water, centrifuged, and the pellet was flash frozen in liquid nitrogen and then kept frozen at -80°C for at least 2 hours. The frozen UCA solution was then lyophilized for 48 hours to remove the aqueous core material, thus resulting in the formation of air-filled hollow microcapsules.

Functionalization of UCA with Targeting Ligand

Once the microbubbles were formed, TRAIL (Sigma-Aldrich, St. Louis, MO) was ligated to the UCA surface using a maleimide reaction⁴⁰⁻⁴¹ with an N-beta-Maleimidopropionic acid hydrazide (BMPH) (Fisher Scientific, Pittsburgh, PA) spacer arm of 0.81 nm in length, using N-(3-Dimethylaminopropyl)-N'-ethylcarbodiimide hydrochloride (EDC) and n-hydroxysulfosuccinimide (NHS), both from Sigma-Aldrich (St. Louis, MO) to activate and catalyze the reactions as seen in Figure 2.

Briefly, 60 mg of UCA were suspended in 4 mL of 0.1 M 2-(N-morpholino)ethanesulfonic acid (MES) buffer (pH 5.2) (Fisher Scientific, Pittsburgh, PA), while the solutions for cross-linking were prepared (14.86 mg BMPH in 1 mL distilled water (dH₂O), 19.17 mg EDC in 1 mL dH₂O, and 12 mg NHS in 1 mL dH₂O). These solutions were added to the UCA suspension, which was then shaken end over end for 30 minutes. Activated UCA were then centrifuged at 5000 rpm (relative centrifugal force 2599.35 g) for 5 minutes and washed to remove unreacted EDC, resuspended in a solution of 1.2 μg TRAIL in 4 mL phosphate buffered saline (PBS), and shaken end over end for 90 minutes. TRAIL-ligated UCA (TRAIL-UCA) were then centrifuged (5000 rpm for 5 minutes), washed 3 times with dH₂O, flash frozen in liquid nitrogen, and lyophilized for 48 hours. In addition to unmodified control UCA, an additional control group was cre-

ated following the ligation procedure, but without the use of chemical cross-linkers EDC and BMPH (non-linker control), to account for the possibility that observed effects were from TRAIL that was only adsorbed to the surface rather than covalently linked. Such adsorbed TRAIL would be easily eluted when contacted with cell cultures, releasing free TRAIL.

Physical and Acoustic Characterization of UCA

Ligated and control groups were morphologically and acoustically evaluated to determine their viability as functionalized UCA. Scanning Electron Microscope (SEM) images were taken with a Philips FEI XL30 Environmental SEM to assess the UCA surface morphology and ensure that the size had not changed substantially during the ligation step. Briefly, 1 mg of UCA was mounted onto an aluminum stub using conductive adhesive tape and sputter coated with platinum-palladium for 40 seconds to prepare for SEM imaging. Three images are taken from a random location on each SEM stub holding the microbubble sample. UCA diameter was measured from these SEM images, using NIH ImageJ image processing software. Briefly, four microbubbles were chosen at random by the researchers from these representative images, the diameters of these microbubbles were measured with ImageJ software, and the results were average for each UCA species. Dose and time response tests were performed in a custom-built acoustic testing system in our lab, using a 5 MHz, 12.7 mm diameter, single element ultrasound transducer (Panametrics, Waltham, MA) spherically focused at a length of 50.8 mm, as described previously.^{5-7,32,34} This transducer was submerged in a bath of distilled water warmed to 37°C and focused through the acoustic window of the custom-built sample vessel filled with 50 mL of warmed (37°C) PBS. A Panametrics Pulsar/Receiver was used to insonate the sample at a pulse repetition frequency (PRF) of 100 Hz. The reflected signals were then received and amplified by 40 dB, fed to a digital oscilloscope (LeCroy, Chestnut Ridge, NY), and analyzed on a computer using a custom LabView program. Baseline readings were taken of the PBS alone, while spinning with a magnetic stir bar, to indicate the amount of background for sample measurements. Then, 3 mg of UCA were suspended in 800 µL of PBS for testing. To determine the cumulative dose response, 20 µL of the UCA suspen-

sion were added to the sample vessel every 30 seconds and the acoustic signal was measured at each time point. Time response, or stability over time while circulating in the US beam, was measured by adding 40 µL of the UCA suspension to the sample vessel with a fresh 50 mL of warmed PBS and the acoustic signal was measured every minute over a period of 15 minutes. These tests were done in triplicate, and the results reported as the average of these readings.

In Vitro Ultrasound-Triggered Nanoshard Generation from UCA

After demonstrating the potential to produce US-triggered n-Sh with the TRAIL-UCA during acoustic tests, UCA were insonated using methods that have been used previously in our lab to generate n-Sh.^{4,36} Briefly, sterile 6-well polystyrene tissue culture plates were clamped at the water-air interface of the acoustic tank described above. The submersible transducer was re-positioned to transmit upward into the wells of the plate, at a distance such that the focal point was within the well. Polyester Transwell membrane inserts (Corning, Lowell, MA) with 400 nm pores (pore density 4×10^6 pores/cm², diameter 24 mm) were inserted into the wells to simulate the leaky vasculature. 5 mg of TRAIL-UCA were suspended in 3 mL of PBS in the bottom of the well, then the Transwell was inserted, and an additional 3 mL of PBS was added on top of the insert. The well was then centered over the transducer at a distance of 50.8 mm (the focal distance of the transducer), and a rubber stopper was placed at the upper level of the fluid in an effort to minimize energy reflection at the liquid-air interface and to prevent standing waves from forming within the sample. The sample was then insonated at a PRF of 100 Hz for 30 minutes, taking 200 µL samples from the upper chamber every 10 minutes for experimental use. Controls were incubated in this setup for 30 min, without insonation.

In Vitro Characterization of Ligated UCA Ability to Induce Cell Death

Finally, *in vitro* studies assess the targeted apoptotic activity induced by the TRAIL-UCA and TRAIL n-Sh. The “supernatant” from the n-Sh tests described above was collected, centrifuged, and then suspended in cell culture media. MDA-MB-231 breast cancer cells were grown to 80% confluence in 48-well plates (to facilitate multiple treatments) in media containing 94% RPMI 1640, 5% FBS, and 1% penicillin/streptomycin antibiotic; 3T3 fibroblasts, representing a TRAIL-resistant group, were grown to 30% confluence based on availability.

Individual batches of both cell types were exposed to seven different treatments representing each treatment vehicle and controls, shown in Table A. Cells were incubated in media containing each treatment for 6 hours, and cell fates were then evaluated using a Live/Dead Cytotoxicity Assay (Invitrogen, Grand Island, NY) and fluorescent microscopy.

Negative Controls	Positive Controls	Test Group 1	Test Group 2
No Treatment	Free TRAIL	Intact Non-linker UCA	Intact TRAIL-ligated UCA
Intact Blank UCA		Non-linker n-Sh (30 mins insonation)	TRAIL-ligated n-Sh (30 mins insonation)

Table A. Treatment groups for *in vitro* cell studies, both TRAIL-sensitive and TRAIL-resistant cell lines.

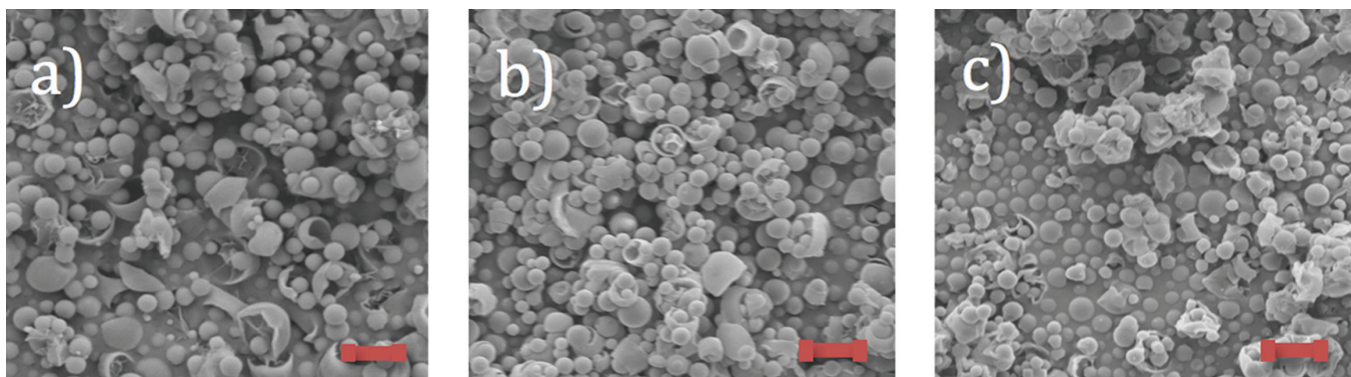


Figure 3. SEM images of UCA. a) Pre-ligation blank UCA. b) Ligated TRAIL-UCA. c) Non-linker control TRAIL-UCA. Accelerating voltage 5 kV, spot size 3, magnification 2500 \times , scale bar 4 μ m.

Images were taken at three random positions throughout each well, and can be considered representative images. Cell fates were counted using customized macros in NIH ImageJ. Briefly, all cells in the image were counted and designated as either live (green) or dead (red). Then, cell death was calculated by determining the percentage of dead cells compared to live cells in these representative images.

Statistical Analysis

Statistical analysis is performed using GraphPad Prism software, where one-way ANOVA analysis is used to determine significance (95% confidence level) and student's t tests are used for individual group comparisons. Error bars represent the Standard Error About the Mean (SEAM).

Results

Physical and Acoustic Characterization of UCA

The resulting TRAIL-UCA and unmodified blank UCA were characterized by evaluating surface morphology before and after modification, as well as acoustic enhancement and stability in the US beam. As shown in Figure 3, SEM images demonstrate that TRAIL attachment does not significantly affect surface morphology as pre- and post-ligation images show smooth, spherical UCA.

Additionally, these SEM images were used to measure UCA diameter, and the results are shown in Figure 4. While the average diameter of blank UCA ($0.871 \pm 0.097 \mu\text{m}$) and non-linker TRAIL-UCA ($0.871 \pm 0.097 \mu\text{m}$) were identical, the SEM images indicate a shift in the size distributions for the non-linker controls. The average diameter of TRAIL-ligated UCA ($1.190 \pm 0.072 \mu\text{m}$) was significantly larger than these controls ($p = 0.0153$). These changes in size can be expected, due to structural modifications being made to the UCA shell during the ligation process. Nonetheless, these agents are within the desired 1 – 2 μ m range for average diameter, and are therefore acceptable for these experiments.

To assess whether the agents retained their function as contrast agents, acoustic enhancement and stability were

assessed. The cumulative dose response results are shown in Figure 5a, where a 5–8 decibel (dB) reduction in maximum enhancement at a value of 12 $\mu\text{g}/\text{mL}$ is seen in the TRAIL-UCA groups when compared to blank PLA controls at the same dose, suggesting that UCA shell properties are altered during maleimide attachment of TRAIL. Despite this modification-induced reduction, both test groups were still able to reflect a clinically-relevant US signal as judged by our previous *in vivo* work,³² suggesting that TRAIL-UCA are still effective contrast agents. In fact, Figure 5b suggests that the process of TRAIL ligation may actually enhance acoustically-triggered n-Sh production, since the stability in the US beam is reduced for these groups compared to the

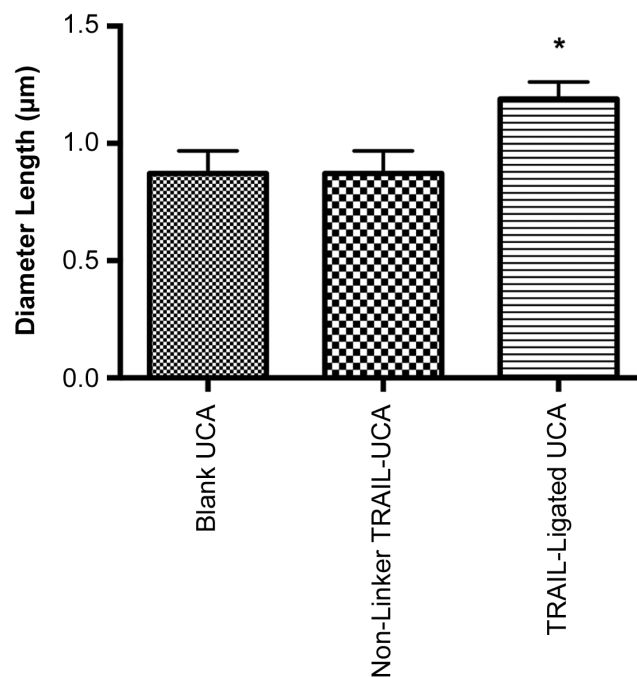


Figure 4. Average UCA diameter, as measured from SEM images. * $p=0.0153$.

blank PLA control. The acoustic half-life, or time until the enhancement signal is halved, is assumed to be due to UCA rupture. For comparison, this half-life was approximately 9 minutes for the ligated TRAIL-UCA and approximately 12 minutes for the surface adsorbed TRAIL-UCA, whereas the half-life of the control blank UCA is greater than 15 minutes. However, there is not a large enough difference between the ligated UCA and non-linker controls ($p > 0.05$) to suggest that the ligation itself has a large effect on the UCA shell properties. Overall, these results suggest that the aqueous environment to which the UCA are exposed during TRAIL attachment modifies the UCA structure, as the SEM images showed no visible change in morphology. The results also indicate that the agents are still capable of functioning as contrast agents that shatter when exposed to US. The larger dose that is required to reach maximum enhancement for TRAIL-UCA is probably due to the fact that a portion of the UCA are destroyed during the ligation process, resulting in a lower concentration of intact UCA.

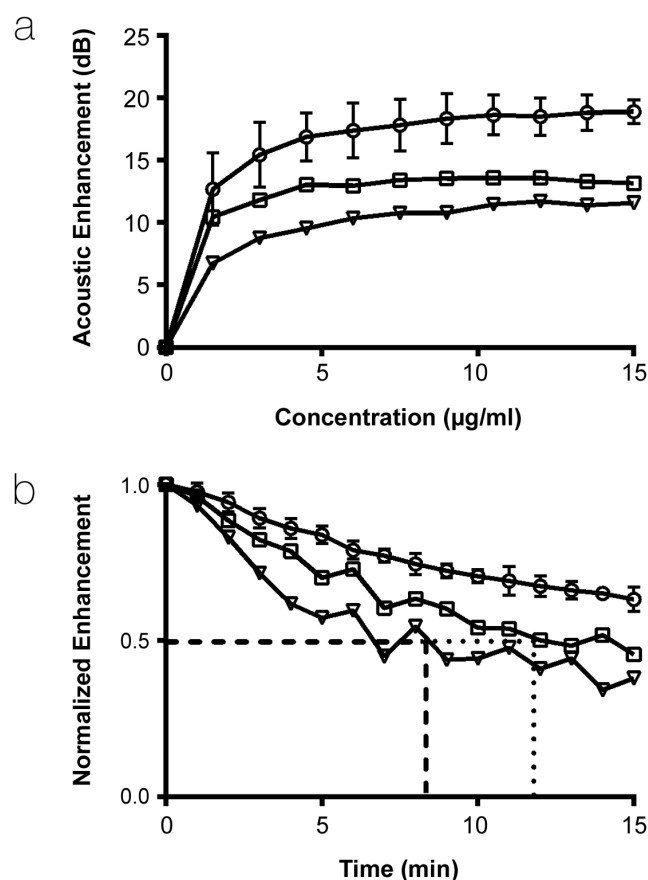


Figure 5. Acoustic evaluation of UCA. a) Acoustic enhancement of each agent, 15 µg/ml doses added and read every 30 seconds, with cumulative enhancement reported in dB. b) Acoustic stability of each agent, normalized to 1, with readings taken every minute, dotted lines indicate half-life of agent. ○ Blank PLA (n = 3), □ Non-linker TRAIL-UCA (n = 1), ▽ Ligated TRAIL-UCA (n = 1).

In Vitro Characterization of Ligated UCA Ability to Induce Cell Death

In the test groups, cells were treated with modified cell culture media consisting of the appropriate intact UCA or n-Sh population suspended in the medium. The treatment groups were: intact non-linker TRAIL-UCA, non-linker n-Sh after 30 minutes of insonation, intact ligated TRAIL-UCA, and ligated n-Sh after 30 minutes of insonation. The control groups were: no treatment (negative control), intact blank PLA UCA (1 mg, negative control), and free TRAIL (10 ng, positive control representing the maximum TRAIL concentration used in the ligation step).

The results from a live/dead assay for the MDA-MB-231 breast cancer cells are shown in Figure 6. As expected, there is little cell death in both negative controls (6a – no treatment, $2.299 \pm 0.347\%$ cell death, and 6b – intact blank UCA, $0.519 \pm 0.216\%$ cell death), while a good deal of cell death ($32.820 \pm 0.796\%$) is evident in the free TRAIL positive control (6c). The cell death is characterized by both the red stained cells and the large black patches, which corresponds to areas where dead cells detached from the plate, with subsequent loss due to washing. For the ligated TRAIL groups, the live/dead assay indicates cell death for both intact UCA ($8.296 \pm 0.169\%$, 6d) and n-Sh ($38.420 \pm 0.020\%$, 6e). It can be observed in Figure 6 that the ligated TRAIL n-Sh were much more effective in inducing cell death in these susceptible cells. In fact, TRAIL-ligated n-Sh induced significantly more cell death than the intact TRAIL-UCA ($p < 0.0001$). Additionally, cell death induced by TRAIL-ligated n-Sh is significantly greater than treatment with free TRAIL ($p = 0.0098$). However, this result could be skewed based on the large patches of lost dead cells. In agreement with our expectations, we saw little cell death in both control non-linker groups (6f – intact non-linker UCA, $2.397 \pm 0.299\%$, and 6g – non-linker n-Sh, $2.020 \pm 1.358\%$), which is not significantly different from the no treatment group ($p = 0.8502$ and $p = 0.8608$, respectively). The non-linker control group results indicate that the observed cell death effects are not incidental events due to release of physically adhered TRAIL, and that the active TRAIL molecules are those that are ligated to the UCA surface.

On the other hand, very little cell death is seen in the TRAIL-insensitive 3T3 fibroblasts, as expected as seen in Figure 7. The 3T3 cells were grown to 30% confluence, and after treatment very few, if any, red-stained dead cells are visible in any of the test groups. For comparison, the free TRAIL group (C) also shows very few dead cells, indicating that TRAIL has no effect on non-sensitive healthy cells. All 3T3 fibroblast samples exhibited less than 3% cell death (actual percentages given in Figure 7) in images collected. In all of these samples, the dark patches represent areas that were never populated with cells, and did not change throughout the experiment.

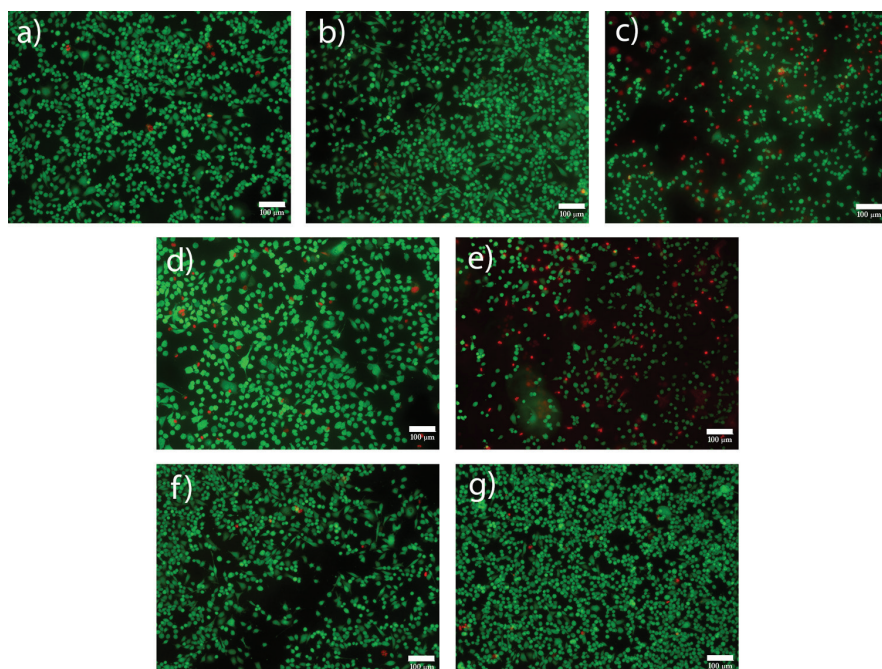


Figure 6. Fluorescent images of MDA-MB-231 human breast cancer cells under various treatments. Green indicates live cells, red indicates dead/apoptotic cells, scale bar 100 μ m. a) no treatment (negative control), b) intact blank PLA UCA (negative control), c) free TRAIL (positive control), d) intact ligated TRAIL-UCA, e) ligated n-Sh, g) intact non-linker TRAIL-UCA, and g) non-linker n-Sh.

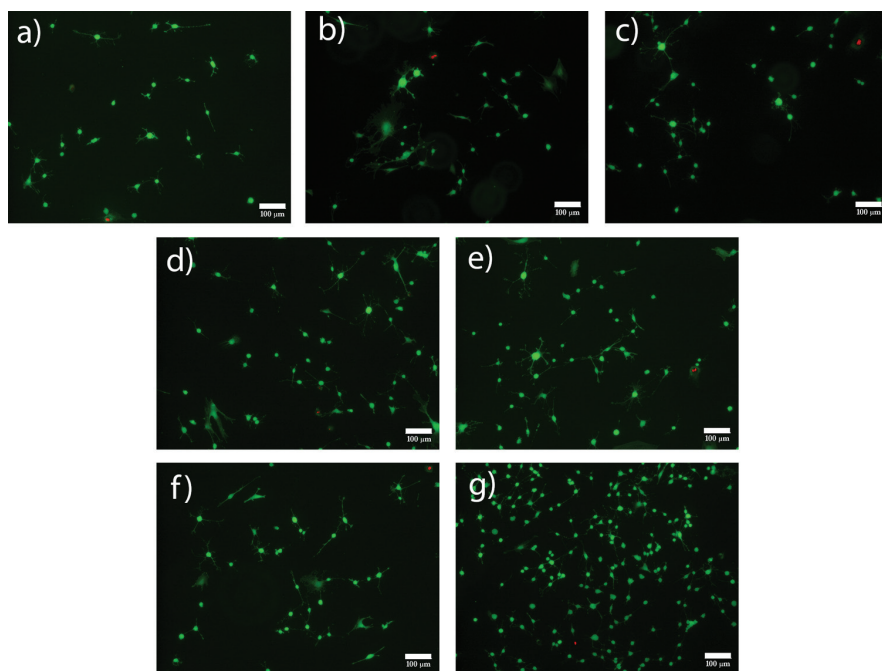


Figure 7. Fluorescent images of 3T3 human fibroblasts under various treatments. Green indicates live cells, red indicates dead/apoptotic cells, scale bar 100 μ m. a) no treatment (negative control, 1.742 \pm 0.076% cell death), b) intact blank PLA UCA (negative control, 2.548 \pm 0.016%), c) free TRAIL (positive control, 1.669 \pm 0.056%), d) intact ligated TRAIL-UCA (2.753 \pm .051%), e) ligated n-Sh (0.799 \pm 0.041%), f) intact non-linker TRAIL-UCA (1.106 \pm 0.031%), and g) non-linker n-Sh (0.659 \pm 0.267%).

Discussion

In this proof of concept study, we have shown that ligation using maleimide chemistry is an effective method for attaching TRAIL to UCA, confirming our preliminary study.^{40,41} We have now shown that these modified UCA maintained acoustic properties and induced cell death in susceptible cells, but not in resistant cells. Importantly, we also show that breast cancer cells treated with n-Sh generated by US treatment of ligated TRAIL-UCA exhibit the greatest extent of cell death among the test groups. This observation is consistent with the hypothesis that shattering a single UCA into n-Sh will produce an abundance of particles that can carry TRAIL to a greater population of susceptible cells than would be available for interaction with a single intact UCA. The added advantages of US interaction with micron-sized particles include radiation force pushing the UCA toward the leaky vasculature wall, UCA rupture due to US-induced inertial cavitation, and cavitation-induced generation of localized mechanical shock waves, microjets, free radicals, localized extreme temperatures (up to 5000 K), transient breaks in the already leaky vasculature,⁴² and US-induced increases in tumor vasculature permeability.⁴³ Combined with these advantages, our results are encouraging for the future of *in situ* generation of nanoparticles. We describe a system utilizing dual-mechanism targeting: first, n-Sh are only generated where the US is focused on the tumor, and second, the surface-bound TRAIL is targeted to cell surface death receptors on cancer cells.

The double emulsion process for UCA manufacture that is described here is also quite versatile for encapsulation of drugs, bioactive molecules, or other species. US-guided delivery of hydrophobic species can be promoted by incorporating the drug into the organic phase, and the same can be said for hydrophilic species if incorporated into the aqueous phase.^{5,34,36,44} One such example that we have studied is encapsulation of doxorubicin (Dox) within the PLA shell, which

has been visualized using confocal microscopy.^{33,34} Drugs such as Dox, 5-fluorouracil, paclitaxel, bortezomib, and actinomycin D have been shown to act synergistically with TRAIL and also to render resistant cancer cells susceptible to TRAIL.^{25,30,45,46} Co-encapsulation of a bioactive molecule, such as bortezomib or doxorubicin, could greatly expand the scope in which these agents can provide effective therapy. Additionally, optimization of the US parameters for n-Sh generation from the functionalized UCA is ongoing. Future studies will further investigate the possibilities for TRAIL-functionalized UCA.

References

1. *Cancer Facts and Figures 2013*, 2013, American Cancer Society: Atlanta, GA.
2. Hobbs, S.K., et al., "Regulation of Transport Pathways in Tumor Vessels: Role of Tumor Type and Microenvironment," *Proc. Natl. Acad. Sci. USA*, Vol. 95, No. 8, 1998, pp. 4607-4612.
3. Jain, R.K., "Delivery of Molecular and Cellular Medicine to Solid Tumors," *Adv. Drug Del. Rev.*, Vol. 64, No. 5, 1997, pp. 353-365.
4. Eisenbrey, J., *Ultrasound Sensitive Polymeric Drug Carriers for Treatment of Solid Tumors*, 2010, Drexel University School of Biomedical Engineering, Science and Health Systems: Philadelphia, PA.
5. Eisenbrey, J., et al., "Ultrasound Triggered Cell Death *in vitro* with Doxorubicin Loaded Poly Lactic-acid Contrast agents," *Ultrasonics*, Vol. 49, No. 8, 2009, pp. 628-633.
6. El-Sherif, D., et al., "Ultrasound Degradation of Novel Polymer Contrast Agents," *J. Biomed. Mater. Res. A*, Vol. 61, No. 2004, pp. 71-8.
7. El-Sherif, D.M. and M.A. Wheatley, "Development of a Novel Method for Synthesis of a Polymeric Ultrasound Contrast Agent," *J. Biomed. Mater. Res. A*, Vol. 66, No. 2, 2003, pp. 347-355.
8. Narayan, P. and M.A. Wheatley, "Preparation and Characterization of Hollow Microcapsules for Use as Ultrasound Contrast Agents," *Polym. Eng. Sci.*, Vol. 39, No. 11, 1999, pp. 2242-2255.
9. Maeda, H. and Y. Matsumura, "Tumorotropic and Lymphotropic Principles of Macromolecular Drugs," *Crit. Rev. Ther. Drug Carrier Syst.*, Vol. 6, No. 3, 1989, pp. 193-210.
10. Maeda, H., "The Enhanced Permeability and Retention (EPR) Effect in Tumor Vasculature: the Key Role of Tumor-Selective Macromolecular Drug Targeting," *Adv. Enzyme Regul.*, Vol. 41, No. 1, 2001, pp. 189-207.
11. Maeda, H., et al., "Tumor Vascular Permeability and the EPR Effect in Macromolecular Therapeutics: a Review," *J. Control. Release*, Vol. 65, No. 1, 2000, pp. 271-284.
12. Iyer, A.K., et al., "Exploiting the Enhanced Permeability and Retention Effect for Tumor Targeting," *Drug Discov. Today*, Vol. 11, No. 17, 2006, pp. 812-818.
13. Jain, R.K., "Barriers to Drug-Delivery in Solid Tumors," *Sci. Am.*, Vol. 271, No. 1994, pp. 58-65.
14. Langer, R., "Drug Delivery and Targeting," *Nature*, Vol. 392, No. 6679 Suppl, 1998, pp. 5-10.
15. Jang, S.H., et al., "Drug Delivery and Transport to Solid Tumors," *Pharm. Res.*, Vol. 20, No. 2003, pp. 1337-50.
16. French, L.E. and J. Tschopp, "The TRAIL to Selective Tumor Death," *Nat. Med.*, Vol. 5, No. 2, 1999, pp. 146-147.
17. Kim, K., et al., "Molecular Determinants of Response to TRAIL in Killing of Normal and Cancer Cells," *Clin. Cancer Res.*, Vol. 6, No. 2000, pp. 335-346.
18. Sanlioglu, A., et al., "Surface TRAIL Decoy Receptor-4 Expression is Correlated with TRAIL Resistance in MCF7 Breast Cancer Cells," *BMC Cancer*, Vol. 5, No. 2005, pp.
19. Shigeno, M., et al., "Interferon-alpha Sensitizes Human Hepatoma Cells to TRAIL-induced Apoptosis Through DR5 Upregulation and NF-kappaB Inactivation," *Oncogene*, Vol. 22, No. 2003, pp. 1653-62.
20. Wang, S. and W.S. El-Deiry, "TRAIL and Apoptosis Induction by TNF-family Death Receptors," *Oncogene*, Vol. 22, No. 2003, pp. 8628-8633.
21. Mitsiades, C.S., et al., "TRAIL/Apo2L Ligand Selectively Induces Apoptosis and Overcomes Drug Resistance in Multiple Myeloma: Therapeutic Applications," *Blood*, Vol. 98, No. 3, 2001, pp. 795-804.
22. Nagane, M., et al., "Increased Death Receptor 5 Expression By Chemotherapeutic Agents in Human Gliomas Causes Synergistic Cytotoxicity With Tumor Necrosis Factor-Related Apoptosis-Inducing Ligand *In Vitro* and *In Vivo*," *Cancer Res.*, Vol. 60, No. 4, 2000, pp. 847-853.
23. Li, Y., et al., "Inducible Resistance of Tumor Cells to Tumor Necrosis Factor-Related Apoptosis-Inducing Ligand Receptor 2-Mediated Apoptosis by Generation of a Blockade at the Death Domain Function," *Cancer Res.*, Vol. 66, No. 17, 2006, pp. 8520-8528.
24. Zhang, Y. and B. Zhang, "TRAIL Resistance of Breast Cancer Cells is Associated With Constitutive Endocytosis of Death Receptors 4 And 5," *Mol. Cancer Res.*, Vol. 6, No. 12, 2008, pp. 1861-1871.
25. Lashinger, L.M., et al., "Bortezomib Abolishes Tumor Necrosis Factor-Related Apoptosis-Inducing Ligand Resistance via A P21-Dependent Mechanism In Human Bladder and Prostate Cancer Cells," *Cancer Res.*, Vol. 65, No. 11, 2005, pp. 4902-4908.
26. Thorburn, A., K. Behbakht, and H. Ford, "TRAIL Receptor-Targeted Therapeutics: Resistance Mechanisms and Strategies To Avoid Them," *Drug Resist Updates*, Vol. 11, No. 1, 2008, pp. 17-24.
27. Tomek, S., et al., "Resistance to TRAIL-Induced Apoptosis in Ovarian Cancer Cell Lines is Overcome By Co-

- Treatment With Cytotoxic Drugs," *Gynecol. Oncol.*, Vol. 94, No. 2004, pp. 107-14.
28. Wahl, H., et al., "Curcumin Enhances Apo2L/TRAIL-induced Apoptosis in Chemoresistant Ovarian Cancer Cells," *Gynecol. Oncol.*, Vol. 105, No. 1, 2007, pp. 104-112.
 29. You, M., et al., "The Combination of ADI-PEG20 and TRAIL Effectively Increases Cell Death in Melanoma Cell Lines," *Biochem. Biophys. Res. Commun.*, Vol. 394, No. 2010, pp. 760-6.
 30. Cuello, M., et al., "Synergistic Induction of Apoptosis by the Combination of TRAIL and Chemotherapy in Chemoresistant Ovarian Cancer Cells," *Gynecol. Oncol.*, Vol. 81, No. 2001, pp. 380-90.
 31. Forsberg, F., et al., "Effect of Shell Type on the In Vivo Backscatter From Polymer-Encapsulated Microbubbles," *Ultrasound Med. Biol.*, Vol. 30, No. 10, 2004, pp. 1281-1287.
 32. Wheatley, M.A., et al., "Comparison of In Vitro and In Vivo Acoustic Response of A Novel 50: 50 PLGA Contrast Agent," *Ultrasonics*, Vol. 44, No. 4, 2006, pp. 360-367.
 33. Eisenbrey, J., et al., "Development and Optimization of A Doxorubicin Loaded Poly (Lactic Acid) Contrast Agent for Ultrasound Directed Drug Delivery," *J. Control. Release*, Vol. 143, No. 1, 2010, pp. 38-44.
 34. Cochran, M.C., et al., "Doxorubicin and Paclitaxel Loaded Microbubbles for Ultrasound Triggered Drug Delivery," *Int. J. Pharm.*, Vol. 414, No. 1, 2011, pp. 161-170.
 35. Cochran, M.C., et al., "Disposition of Ultrasound Sensitive Polymeric Drug Carrier in a Rat Hepatocellular Carcinoma Model," *Acad. Radiol.*, Vol. 18, No. 11, 2011, pp. 1341-1348.
 36. Eisenbrey, J., M. Soulen, and M. Wheatley, "Delivery of Encapsulated Doxorubicin by Ultrasound-Mediated Size Reduction Of Drug-Loaded Polymer Contrast Agents," *IEEE Trans. Biomed. Eng.*, Vol. 57, No. 2010, pp. 24-8.
 37. Arvanitis, C.D., et al., "Cavitation-Enhanced Extravasation for Drug Delivery," *Ultrasound Med. Biol.*, Vol. 37, No. 2011, pp. 1838-52.
 38. Bekeredjian, R., et al., "Ultrasound Targeted Microbubble Destruction Increases Capillary Permeability in Hepatomas," *Ultrasound Med. Biol.*, Vol. 33, No. 10, 2007, pp. 1592-1598.
 39. Geers, B., et al., "Crucial Factors and Emerging Concepts In Ultrasound-Triggered Drug Delivery," *J. Control. Release*, Vol. 164, No. 2012, pp. 248-255.
 40. Oum, K., *Therapeutic and Diagnostic Applications of Ultrasound Contrast Media for Breast, Ovarian and Skin Cancers*, 2008, Drexel University School of Biomedical Engineering, Science and Health Systems: Philadelphia, PA.
 41. Wheatley, M.A., et al., "Cellular Signal Transduction can be Induced by TRAIL Conjugated to Microcapsules," *J. Biomed. Mater. Res. A*, Vol. 100, No. 10, 2012, pp. 2602-2611.
 42. Forbes, M., R. Steinberg, and W. O'Brien Jr., "Examination of Inertial Cavitation of Optison in Producing Sonoporation of Chinese Hamster Ovary Cells," *Ultrasound Med. Biol.*, Vol. 34, No. 2008, pp. 2009-2018.
 43. Stieger, S.M., et al., "Enhancement of Vascular Permeability With Low-Frequency Contrast-Enhanced Ultrasound in the Chorioallantoic Membrane Model," *Radiology*, Vol. 243, No. 1, 2007, pp. 112-121.
 44. Lathia, J.D., et al., "Surface Modification of Polymeric Contrast Agents for Cancer Targeting," *Pharm. Engr.*, Vol. 24, No. 1, 2004, pp. 92-103.
 45. Keane, M.M., et al., "Chemotherapy Augments TRAIL-induced Apoptosis in Breast Cell Lines," *Cancer Res.*, Vol. 59, No. 3, 1999, pp. 734-741.
 46. Yamanaka, T., et al., "Chemotherapeutic Agents Augment TRAIL-Induced Apoptosis in Human Hepatocellular Carcinoma Cell Lines," *Hepatology*, Vol. 32, No. 3, 2000, pp. 482-490.

Acknowledgments

The authors wish to acknowledge several contributors to this research project. We thank Dr. Michael Cochran for preparing the breast cancer cells and help with preparation of figures, and Dr. Nicola Francis for assistance with cell staining techniques and fluorescent microscopy training. Dolores Conover is thanked for preparing the fibroblast cells. The authors received research support from the Drexel University Students Tackling Advanced Research (STAR) Program, the Drexel University Office of Undergraduate Research, and National Institutes of Health (NIH) Grant HL52901.

About the Authors



Lauren Jablonowski did her undergraduate work at Drexel University where she earned a bachelor's and master's degree in biomedical engineering, and is currently a PhD candidate focusing on polymer ultrasound contrast agents for targeted drug and bioactive molecule delivery. Academic achievements include being named a Drexel University Calhoun Scholar, the 2009 Drexel Panhellenic Council Scholar of the Year, and graduating magna cum laude from Drexel University and with distinction from Drexel's Pennoni Honors College. She is a member of ISPE, Tau Beta Pi Engineering Honor Society, and Delta Phi Epsilon. She can be contacted by email: lj62@drexel.edu.

Drexel University, School of Biomedical Engineering, Science and Health Systems, 3141 Chestnut St., Philadelphia, Pennsylvania 19104, USA.



Averie Palovcak is currently an undergraduate student at Drexel University studying biomedical engineering. Through the STAR Scholar undergraduate research program at Drexel University, she has assisted in developing ultrasound contrast

agents for targeted drug delivery in cancer therapy. As part of the cooperative education experience at Drexel University, she also has worked with the Department of Radiation Oncology at the University of Pennsylvania researching proton therapy. Her academic achievements include invitations to the National Collegiate Research Conference at Harvard University and at the Colonial Academic Alliance Undergraduate Research Conference. She can be contacted by email: amp389@drexel.edu.

Drexel University, School of Biomedical Engineering, Science and Health Systems, 3141 Chestnut St., Philadelphia, Pennsylvania 19104, USA.



Dr. Margaret Wheatley received her undergraduate degree in chemistry honors from Oxford University, a master's degree from the same university in biochemistry, and her PhD in chemical engineering and applied chemistry from the University

of Toronto, Canada in 1982. She completed post-doctoral research in the Department of Applied Biology at the Massachusetts Institute of Technology, and after a three-year experience in industry in the advanced drug delivery group at Glaxo Smith Kline, joined the Drexel faculty in 1987. Her research employs an engineering approach combined with knowledge of biology and polymer chemistry to solve problems of mass transport and delivery in biological systems, with special emphasis on cancer diagnosis and treatment. Her laboratory is an eclectic mix encompassing the use of biodegradable polymers to stabilize microbubbles of inert gas for ultrasound imaging, in situ ultrasound-activated generation of drug-loaded nano particles for solid tumor chemotherapy and development of multi-modal theranostics. In the area of tissue engineering, she is developing smart scaffolds for spinal cord repair.

Drexel University, School of Biomedical Engineering, Science and Health Systems, 3141 Chestnut St., Philadelphia, Pennsylvania 19104, USA. 